Δελτίο Ελληνικής Γεωλογικής Εταιρίας τομ. XXX/5, 123-136, 1994
Πρακτικά 7ου Επιστημονικού Συνεδρίου, Θεσσαλονίκη, Μάιος 1994
Bulletin of the Geological Society of Greece vol. XXX/5, 123-136, 1994
Proceedings of the 7th Congress, Thessaloniki, May 1994

TIME DEPENDENT SEISMICITY IN THE ALPINE-HIMALAYAN BELT

B. Papazachos, G. Karakaisis, E. Papadimitriou, T. Tsapanos and Ch. Papaioannou

ABSTRACT

The Alpine-Himalayan belt is divided in 143 seismogenic sources and the interevent times of strong shallow mainshocks in each source were considered. The estimated 731 interevent times were used to determine the following relations:

$$\log T_t = 0.19\, M_{min} + 0.32\, M_p - 0.43 \log m_o + 8.90$$

$$M_f = 0.88\, Mmin - 0.30\, M_p + 0.43 \log m_o - 7.54$$

where Tt is the interevent time, measured in years, Mmin the surface wave magnitude of the smallest mainshock considered, Mp the magnitude of the preceding mainshock, mo the moment rate in each source per year. Based on these relations and taking into account the time of occurrence and the magnitude of the last mainshock in each seismogenic source, time dependent conditional probabilities for the occurrence of the next large (Ms≥7.0) shallow mainshocks in the next ten years and the magnitudes of the expected mainshocks are determined for each source.

ΠΕΡΙΛΗΨΗ

Η Ευρασιατική σεισμική ζώνη χωρίσθηκε σε 143 σεισμογόνες πηγές και υπολογίστηκαν οι χρόνοι επανάληψης των ισχυρών επιφανειακών σεισμών σε κάθε πηγή. Οι 731 χρόνοι επανάληψης που βρέθηκαν, χρησιμοποιήθηκαν για τον υπολογισμό των παρακάτω σχέσεων:

$$\log T_t = 0.19\, M_{min} + 0.32\, M_p - 0.43 \log m_o + 8.90$$

$$M_f = 0.88\, M_{min} - 0.30\, M_p + 0.43 \log m_o - 7.54$$

όπου T_t είναι οι χρόνοι επανάληψης σε έτη, M_{min} το επιφανειακό μέγεθος του μικρότερου κύριου σεισμού που λήφθηκε υπόψη, M_p το μέγεθος του προηγούμενου κύριου σεισμού, M_f το μέγεθος του επόμενου κύριου σεισμού και mo ο ετήσιος ρυθμός έκλυσης σεισμικής ροπής σε κάθε πηγή. Με βάση αυτές τις σχέσεις και λαμβάνοντας υπόψη το χρόνο γένεσης και το μέγεθος του τελευταίου κύριου σεισμού σε κάθε πηγή, υπολογίσθηκαν οι πιθανότητες γένεσης των μελλοντικών πολύ ισχυρών (M_s≥7.0) επιφανειακών κύριων σεισμών σε κάθε πηγή, καθώς και το μέγεθος των σεισμών αυτών.

Laboratory of Geophysics, University of Thessaloniki, Thessaloniki GR54006, Greece.

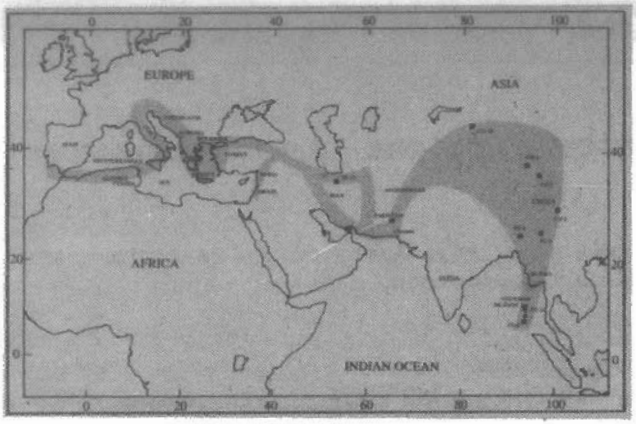

Fig. 1: The shaded area corresponds to the Alpine-Himalayan belt that has been studied in the present paper. Solid squares denote the centers of the seismogenic sources that have been assigned with high probabilities (≥0.5) for the generation of large earthquakes (Ms≥7.0) during the next 10 years (1994-2003).

INTRODUCTION

Current research on seismicity patterns is mainly focused, among other aspects, on the nature of earthquake recurrence. The results of this research have been expressed by means of two alternative representations for earthquake recurrence patterns, namely, the time-predictable model and the slip-predictable model (Bufe et al., 1977; Shimazaki and Nakata, 1980; Sykes and Quittmeyer, 1981). According to the first of these models, the earthquake recurrence interval and the size of the preceding main shock in a certain seismic source are positively correlated whereas according to the second model, the size of the next main shock depends on the time elapsed since the last main shock.

In an attempt to resolve the nature of earthquake recurrence Papazachos (1988a, b, 1989, 1992, 1993) proposed a model in which the interevent time and the magnitude of the following main shock were quantitatively expressed in terms of the magnitude of the smallest main shock considered and the magnitude of the preceding main shock in a certain seismogenic source. Each source may include, in addition to the main fault where the characteristic earthquake is generated, other smaller faults where smaller main shocks also occur. This model was subsequently improved by taking into account the yearly released seismic moment in each seismogenic source (Papazachos and Papaioannou, 1993) and has already been applied in several areas of the world (Papadimitriou, 1993; Panagiotopoulos, 1994; Karakaisis, 1994a, b). In a very recent paper concerning the circum-Pacific convergent belt, the applicability of the time and magnitude predictable model has been tested with encouraging results (Papazachos et al., 1994).

In the present paper the test is extented to the second major deforming zone, the Alpine-Himalayan belt (Fig. 1). Furthermore, probabilities for the generation of large earthquakes during the next 10 years (1994-2003) in seismogenic sources in this belt are determined.

THE SEISMOGENIC SOURCES

The active tectonics of the Alpine-Himalayan belt or of some of its segments, have been studied in detail by many authors (McKenzie, 1972; Nowroozi, 1971; Kaila et al., 1972; Molnar and Tapponnier, 1978; Quittmeyer and Jacob, 1979; Jackson and McKenzie, 1984, 1988; Anderson and Jackson, 1987; Buforn et al., 1988; Papazachos, 1990, among others).

For the purpose of the present study the western Mediterranean (southern Spain, NW Africa) has been divided into five seismogenic sources on the basis of the spatial distribution of seismicity, of focal mechanisms and of observations on the surface (Buforn et al., 1988;

Dewey, 1990; Kiratzi and Papazachos, 1994).

The shallow seismic activity in Italy is concentrated along the Apennines mountain chain and in eastern Alps (Anderson and Jackson, 1987). The separation of Italy into six discrete seismogenic sources (Karakaisis, 1993) was mainly based on the contour mapping of seismic activity concerning events with M≥4.0 that occurred in Italy during 1900-1986 (Mulargia et al., 1987), as it is depicted in a more recent work (Gasperini and Mulargia, 1992, p. 423). The stronger shallow earthquakes of the present century occurred at the southern part of Italy.

Recent strong earthquakes have been concentrated in two main zones in Yugoslavia. The most northerly cluster of seismicity occurs south of Zagreb near the Sava river, whereas the southern Dalmatian coast is the most seismically active area of Yugoslavia, with earthquakes occurring in a band approximately 100 Km wide which runs south from near Split towards Albania (Anderson and Jackson, 1987; Jackson and McKenzie, 1988).

The Aegean area, which exhibits the highest seismic activity of western Eurasia, includes the Hellenic arc, the Aegean Sea and the surrounding areas (Greece, Albania, southern Yugoslavia, southern Bulgaria, NW Turkey) and has been separated in a number of seismogenic sources (Papazachos, 1990, 1992; Papazachos and Papaioannou, 1993). This separation has been done on the basis of spatial clustering of epicenters of strong earthquakes, seismicity level, maximum earthquake observed, type of faulting, geomorphological features, etc.

Active tectonics in Turkey are manifested by high seismic activity along North and East Anatolian strike-slip Fault Zones. During the present century both faults have repeatedly been ruptured, causing heavy damage in Anatolia and SE Turkey. Most of the seismogenic sources were mainly defined on the basis of the rupture lengths of the stronger earthquakes that occurred in these zones (Ambraseys, 1970; Barka and Kadinsky-Cade, 1988), as well as on certain seismological criteria (Karakaisis, 1994a).

The Dead Sea transform fault system, which runs along the eastern coasts of the Mediterranean Sea and forms the plate boundary that links the Arabian plate convergence in southern Turkey with the active seafloor spreading in the Red Sea (Ambraseys and Barazangi, 1989), has been divided into two seismogenic sources. The meizoseismal region of the earthquake of 20 May 1202 defines the first seismogenic source (Ambraseys and Melville, 1988), while a spatial cluster of strong earthquakes that occurred in the Syrian-Turkish border region defines the second source.

Iran is a country of diverse seismicity, ranging from low to moderate seismicity in central and southern Iran to high seismicity in northwestern, northern and eastern Iran. The whole area has been divided into 21 seismogenic sources (Karakaisis, 1994b) on the basis of the distribution of macroseismic intensities (Ambraseys and Melville, 1982) and the locations of fault breaks or earthquake faults studied by many authors (see Karakaisis, 1994b, and references therein). Further to the east, several seismogenic sources have been defined and correspond to the eastern section of the Makran system, the Ornach Nal and the Chaman fault systems (Quittmeyer, 1979; Jackson and McKenzie, 1984), the Herat fault in northeastern Afghanistan (Quittmeyer and Jacob, 1979) and the Yasman fracture zone (Kaila et al., 1974).

China and its surroundings, being one of the most active tectonic regions of the world, exhibits seismicity that is spread diffusely over almost the whole region. This seismic activity has its origin in the continued convergence of India and Eurasia (Molnar and Tapponnier, 1975). The definition of the

seismogenic sources (Tsapanos and Papazachos, 1994), was based on the seismotectonic studies of Tapponnier and Molnar (1977) and Molnar and Tapponnier (1978), and on the map of Zhang and Chen (1989) that depicts structural features of China derived from Landsat I and II images. The southeasternmost seismogenic sources of the area studied in the present paper include Andaman and Nicobar islands (Kaila et al., 1972).

METHOD AND DATA

Papazachos and Papaioannou (1993), based on interevent times of strong shallow main shocks that occurred in seismogenic sources in the Aegean area, proposed the following relations which are the essence of the time and magnitude predictable model:

$$\log T_t = b M_{min} + c M_p + d \log m_o + t \qquad (1)$$

$$M_f = B M_{min} + cM_p + D \log m_o + m \qquad (2)$$

where Tt is the calculated interevent time, M_{min} is the cut-off main shock magnitude in a certain source, M_p and Mf are the magntitudes of the preceding and the following main shocks and m_o is the yearly moment rate in this source. b, c, d, t, B, C, D, and m are the parameters to be determined by using all the available data from all sources. m_o, being a measure of seismicity level, can be reliably calculated if enough data are available for the source which may concern not only the few main shocks but all the earthquakes, above certain cut-off magnitude to ensure completeness, that occurred in the source. Thus, according to Molnar's method (1979), the relative number of events with seismic moment, M_o, equal to or larger than a certain value, is given by the relation:

$$N(M_o) = G.M_o^{-E} \qquad (3)$$

where

$$G = 10^{(a + \frac{bk}{r})} \quad and \quad E = \frac{b}{r} \qquad (4)$$

with a, b, being the constants of the Gutenberg and Richter's recurrence law (1944):

$$\log N = a - bM \qquad (5)$$

normalized for one year, while r, k, are the parameters of the moment-magnitude relation:

$$\log M_o = rM + k \qquad (6)$$

proposed by Kanamori (1977). r and k are equal to 1.5 and 16.1, respectively. The yearly rate of the seismic moment release is given by the relation:

$$m_o = \frac{G}{1-E} M_{o,max}^{1-E} \qquad (7)$$

where $M_{o,max}$ is the seismic moment released by the larger earthquake in the source.

The determination of the parameters of the relations (1) and (2) has been

done by a computer code, written by C. Papazachos, which is based on a well-known multilinear regression technique (Draper and Smith 1966; Weisberg, 1980).

The data used for each seismogenic source concern the interevent time, T, measured in years, between successive main shocks with magnitudes M_p and M_F, which are equal to or larger than a certain cut-off main shock magnitude, M_{min}. Considering, for example, n main shocks in the source we calculate interevent times, T, between successive main shocks with magnitudes equal to or larger than the smaller main shock magnitude, M_{min1}. Then, the second smaller main shock magnitude, M_{min2} ($>M_{min1}$) is considered and new interevent times between successive main shocks with magnitudes equal to or larger than Mmin2 are calculated. This procedure is continued until the last $M_k \leq M_{max}$, with k=n-1, is considered as an M_{mink} for the respective seismogenic source.

The magnitudes M_p and M_F, and for that matter, the M_{min}, are not the actual surface wave magnitudes of the main shocks but the cumulative magnitudes of each seismic sequence, that is, the magnitudes that correspond to the total seismic moment released by the major shocks (the main shock and its larger foreshocks and aftershocks) of the sequence and which have been calculated by the relation (5).

The terms "foreshock, aftershock", are meant in their broad sense and concern earthquakes that occur during certain time intervals before and after the larger earthquakes in a certain seismogenic source. This is because the model applied aims at predicting the main shocks in the source, i.e. strong earthquakes that occur at the beginning and the end of each seismic cycle and not smaller earthquakes that occur during the preseismic and postseismic activations. In this way, the earthquakes that have been considered as "foreshocks" are in accordance with Mogi (1985) who suggested that seismic activity over a wide area would increase through a rise in crustal stress and that these shocks are foreshocks in their broad sense. The same author suggested also that, according to the time predictable model, the duration of the preseismic activity is constant. Regarding this topic, recent studies on the seismic cycle showed that the last phase of the seismic cycle is characterized by an accelerated activity period with a fairly constant duration of 2.7 ± 0.6 years (Karakaisis et al., 1991), which culminates before the second main shock of the seismic cycle and does not depend on the magnitudes of the first or the second main shock. This duration of foreshock activity has been taken into account in the present study.

Mogi (1985) also suggested that according to the same model the duration of the postseismic activity depends on the magnitude of the preceding main shock. Recently Papazachos et al. (1994), based on circum-Pacific data, proposed the following relation between the duration, t(in years), of the aftershock activity and the magnitude, M, of the main shock, which has been used in the present study:

$$\log t = 0.006 + 0.13\, M \qquad (8)$$

Information on the focal parameters of the earthquakes used in the present study comes from various sources that are cited in the papers mentioned in the previous section of the paper. Additional information comes from the catalogues of Pacheco and Sykes (1992), Abe (1981, 1984), Abe and Noguchi (1983), Tsapanos et al., (1990) and from the ISC and NEIC monthly bulletins.

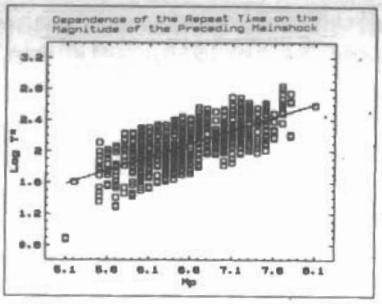

Fig. 2: Dependence of the interevent time on the magnitude of the preceding main shock.

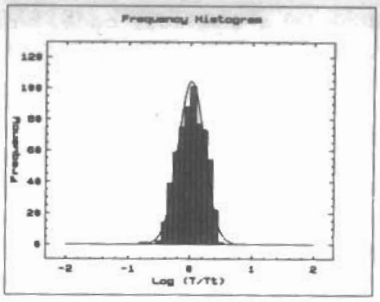

Fig. 3: The frequency distribution of the logarithm of the ratio of the observed interevent times to the theoretically calculated ones.

RESULTS

The data sample consists of 731 observations (T, Mp, MF, Mmin) that come from 143 seismogenic sources. Howevere, some of these observations are not very reliable and were progressively discarded during the multilinear regression, since they presented the larger standard deviations from their mean value, z. Thus, from the remaining 607 observations belonging in the $z \pm 1.6$ s.d. interval, the following relation was derived:

$$log\ T_t = 0.19\ M_{min} + 0.32\ M_p - 0.43\ log\ M_o + 8.90 \quad (9)$$

with a multilinear correlation coefficient, R, equal to 0.73 and a standard deviation equal to 0.20. Figure 2 depicts a plot of the quantity $logT^*=logT-0.19M_{min}+0.43logm_o-8.90$ as a function of the magnitude of the preceding main shock, M_p, where T, M_{min}, $logm_o$ and M_p are the observed quantities. The line drawn is the least squares' fit. Figure 3 shows the frequency distribution of the quantity $log(T/T_t)$, which is fitted by a normal distribution with z=0.0 and s.d.=0.20.

Following a similar procedure, the values of the parameters B, C, D, and m of the relation (2) were determined by all available observations and the following relation was found:

$$M_f = 0.88\ M_{min} - 0.30\ M_p + 0.43\ log\ m_o - 7.54 \quad (10)$$

with R=0.82 and s.d.=0.38. Figure 4 shows the frequency distribution of the quantity M_F-M_f, that is, the difference between the observed magnitude of the following main shock, M_F, and the calculated magnitude of the expecting main shock, M_f, by the relation (9). This is fitted by a normal distribution with z=0.0 and s.d.=0.38.

PREDICTION OF THE NEXT LARGE SHALLOW MAIN SHOCK IN SEISMOGENIC SOURCES OF THE ALPINE-HIMALAYAN BELT

The estimation of the time of occurrence of the next main shock and its magnitude in a seismogenic source seems now an easy task, if one makes use of the equations (8) and (9), taking into account the time of occurrence and the magnitude of the last main shock in this source. It is better, however, to

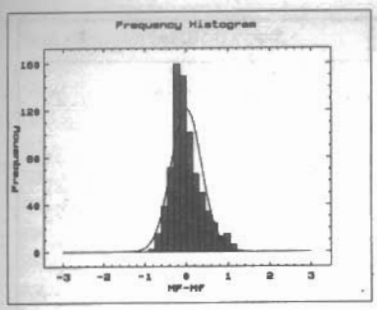

Fig. 4: The frequency distribution of the difference between the observed magnitudes, M_F, of the following main shocks and the calculated ones, M_f.

estimate the probability of occurrence of a next main shock larger than a certain cut-off magnitude and in a certain time interval, because there is considerable fluctuation of the observed interevent times, T, in respect to the interevent times, Tt, calculated by the equation (8), as it can be seen in Figs. 2 and 3.

Since it has been proved that the quantity T/Tt follows a lognormal distribution and assuming that this holds for each source separately, the probabilities of occurrence of a shallow main shock with Ms≥7.0 during the next 10 years (1994-2003) are calculated. Table I gives information on the highest probabilites, P10, of occurrence of large main shocks in the next 10 years and the magnitude, Mf, of the expecting main shock in each source, as it has been calculated by the relation (9). As an error in the magnitude determination of the expecting earthquake, a±1 s.d. may be considered, that is, 0.4 magnitude units.

It can be seen from Table 1 that 10 sources in Asia (Iran, Pakistan-Afghanistan, China, Andaman-Nicobar islands) are assigned with wigh probabilities for the generation of large (Ms≥7.0) earthquakes during the next 10 years.

Table 1: Information on the expected shallow mainshocks. Epicentre coordinates, φ, λ, and the corresponding uncertainties, σ, the expected magnitudes, M_f, and the corresponding probabilities, P10, for the occurrence of large (Mmin≥7.0) shallow mainshocks during the period 1994-2003 along the Alpine-Himalayan Belt.

Seismogenic Source		φ°N	±σ	λ°E	±σ	M_f	P_{10}
SP-1	Terceira	36.75	1.18	-10.2	0.37	7.3	0.40
SP-2	Seville	36.19	0.59	-6.71	0.45	7.3	0.44
SP-3	Granada	36.29	0.95	-3.40	0.95	--	—
NA-1	Algeria	36.31	0.38	1.79	1.11	7.2	0.12
NA-2	Tunisia	35.66	0.90	10.07	1.22	--	--
IT-1	Friuli	46.32	0.07	12.67	0.47	7.1	0.30
IT-2	East Coasts	4.00	0.80	13.08	0.75	--	--
IT-3	Bologna	43.84	0.89	10.68	1.10	--	--
IT-4	Roma	42.35	0.93	12.63	1.51	7.2	0.22
IT-5	Napoli	40.92	0.20	15.46	1.30	7.0	0.26
IT-6	Messina	38.34	0.26	14.80	0.75	7.5	0.32
YU-1	Split-Dalmatia	43.52	0.40	16.40	0.49	--	--
YU-2	Zagreb-Sava River	45.17	0.19	17.67	0.47	--	--
GR-1	Montenegro	42.07	0.33	19.24	0.72	7.0	0.03
GR-2	Dirrachio	41.14	0.34	19.65	0.49	--	--
GR-3	Avlona	40.38	0.61	19.68	0.20	--	--
GR-4	Igoumenitsa	39.72	0.50	20.29	0.64	--	--
GR-5	Preveza	39.04	0.24	20.84	0.44	--	--
GR-6	Lefkada	38.81	0.16	20.56	0.15	--	--
GR-7	Cephalonia	38.33	0.32	20.58	0.42	7.3	0.33

Seismogenic Source		$\varphi^{\circ}N$	$\pm\sigma$	$\lambda^{\circ}E$	$\pm\sigma$	M_f	P_{10}
GR-8	Zakynthos	37.86	0.27	20.90	0.31	7.3	0.27
GR-9	Ionian Sea 1	37.61	0.42	20.31	0.54	--	--
GR-10	Pylos	37.07	0.26	21.60	0.48	7.5	0.34
GR-11	Mani	36.45	0.37	22.27	0.09	7.3	0.20
GR-12	NW of Crete	35.85	0.41	22.80	0.14	7.5	0.23
GR-13	Ionian Sea 2	36.89	0.42	20.94	0.74	--	--
GR-14	Ionian Sea 3	35.60	1.02	22.20	0.86	--	--
GR-15	SW of Crete	35.11	0.24	23.84	0.80	7.3	0.27
GR-16	SE of Crete	34.89	0.16	25.91	0.71	--	--
GR-17	Sea of Libya 1	34.66	0.32	24.12	1.16	7.2	0.23
GR-18	Sea of Libya 2	34.43	0.17	25.33	0.79	--	--
GR-19	Karpathos	35.44	0.29	27.26	0.56	7.5	0.21
GR-20	Rhodos	36.15	0.29	28.23	0.46	--	--
GR-21	Marmaris	36.13	0.54	29.05	0.75	7.3	0.17
GR-22	Stravo 1	34.67	0.62	26.73	0.68	--	--
GR-23	Stravo 2	35.41	0.22	27.83	0.23	7.3	0.26
GR-24	Elbasan	41.33	0.39	20.28	0.28	--	--
GR-25	Tepeleni	40.57	0.38	20.00	0.00	--	--
GR-26	Maliq	41.67	0.52	20.70	0.28	--	--
GR-27	Ochrida	40.88	0.32	20.70	0.13	--	--
GR-28	Jannena	39.80	0.60	20.95	0.50	--	--
GR-29	Karpenissi	39.10	0.00	21.60	0.20	--	--
GR-30	Megalopolis	37.60	0.32	22.08	0.17	--	--
GR-31	Kalamata	37.10	0.14	22.12	0.26	--	--
GR-32	Sparti	36.70	0.00	22.45	0.10	--	--
GR-33	Kythera	35.87	0.41	23.23	0.41	--	--
GR-34	Sitia	35.54	0.37	26.14	0.53	--	--
GR-35	Sea of Karpathos	36.10	0.00	26.85	0.10	--	--
GR-36	Simi	36.44	0.19	27.48	0.52	--	--
GR-37	Patra	38.38	0.23	21.74	0.20	--	--
GR-38	W. Corinthiakos	38.29	0.24	22.31	0.34	7.3	0.28
GR-40	Methana	37.67	0.25	23.20	0.00	--	--
GR-41	Milos	36.95	0.30	24.65	0.30	--	--
GR-42	Santorini	36.66	0.24	25.74	0.84	6.9	0.13
GR-43	Kos	36.67	0.17	27.08	0.30	--	--
GR-44	Alicarnassos	37.07	0.23	28.30	0.53	7.3	0.26
GR-45	Denisli	37.23	0.34	29.50	0.59	7.2	0.18
GR-46	Thessalia	39.33	0.25	22.67	0.65	7.3	0.35
GR-47	N. Evoikos	38.73	0.25	23.05	0.43	7.2	0.23
GR-48	S. Evoikos	38.28	0.07	23.40	0.42	7.1	0.25
GR-49	Samos	37.82	0.31	26.99	0.47	7.2	0.21
GR-50	Aidin	37.83	0.36	29.26	0.95	7.3	0.30
GR-51	Psara	38.41	0.10	25.28	0.29	--	--
GR-52	Chios	38.39	0.36	26.29	0.26	--	--
GR-53	Ismir	38.42	0.28	27.43	0.78	--	--
GR-54	Alasehir	38.33	0.25	29.97	1.11	--	--
GR-55	Skopelos	39.43	0.64	23.81	0.59	7.1	0.06
GR-56	Ag. Efstratios	39.37	0.39	24.87	0.78	7.1	0.19
GR-57	Lesbos	39.11	0.40	26.06	1.26	7.1	0.07
GR-58	Demirci	39.27	0.42	28.00	0.74	7.3	0.33

Seismogenic Source		φ°N	±σ	λ°E	±σ	M_f	P_{10}
GR-59	Gediz	39.16	0.39	29.44	0.70	7.2	0.28
GR-60	Hellispontos	40.39	0.55	27.17	0.77	7.6	0.37
GR-61	Prussa	40.32	0.66	29.00	0.79	7.3	0.47
GR-62	Athos	40.17	0.24	24.70	0.53	7.3	0.24
GR-63	Samothraki	40.44	0.10	25.94	0.52	--	--
GR-64	Volvi	40.63	0.31	23.50	0.62	7.2	0.28
GR-65	Doirani	41.15	0.31	22.58	0.50	--	--
GR-66	Skopje	42.15	0.30	21.40	0.00	--	--
GR-67	Drama	41.18	0.15	24.24	0.63	7.5	0.24
GR-68	Kresna	41.97	0.24	23.19	0.59	7.7	0.34
GR-69	Philippoupolis	42.16	0.10	25.22	0.75	7.0	0.27
TU-1	Adaparazi	40.60	0.90	30.49	0.50	7.2	0.29
TU-2	Bolu	40.74	0.68	32.15	1.15	7.1	0.28
TU-3	Tosya	40.73	0.64	35.06	1.75	7.7	0.39
TU-4	Erzincan	40.11	0.50	38.42	1.34	7.4	0.37
TU-5	Karliova	39.41	0.39	40.84	0.86	7.2	0.31
TU-6	Erzurum	40.30	0.58	42.14	0.77	7.2	0.12
TU-7	Bingol	38.75	0.48	39.98	0.85	7.1	0.25
TU-8	Malatya	38.10	0.41	38.43	0.74	7.3	0.25
ME-1	DSFT	33.00	1.70	35.66	0.70	7.5	0.23
ME-2	Latakya	35.85	1.15	36.40	0.74	7.2	0.38
IR-1	Silakhor	33.49	0.79	47.71	0.45	7.6	0.42
IR-2	Izeh-Andika	31.67	0.54	49.67	0.47	--	--
IR-3	Central Zagros	29.87	0.14	50.97	0.07	--	--
IR-4	Qir-Karzin	28.12	0.28	53.33	0.82	7.1	0.14
IR-5	Southern Zagros	27.93	0.30	54.30	0.46	--	--
IR-6	Khurgu	27.63	0.18	55.96	0.07	7.2	0.17
IR-7	Salmas	37.55	0.45	44.50	0.50	7.6	0.32
IR-8	Maku Ararat	39.73	0.71	43.57	0.91	7.2	0.22
IR-9	Tabriz	38.15	0.63	46.28	0.82	7.5	0.27
IR-10	Khalhal	38.00	0.22	48.97	0.05	--	--
IR-11	Manjil	36.90	0.14	49.83	1.18	7.1	0.00
IR-12	Buyin-Zahra	36.09	0.77	49.01	1.57	6.9	0.07
IR-13	Tash-Shahrud	36.30	0.37	53.25	0.43	7.7	0.61
IR-14	Central Alburz	35.19	0.64	53.60	1.50	--	--
IR-15	Kopet-Dag	37.50	0.79	58.15	0.85	7.3	0.45
IR-16	Turshiz	35.30	0.67	59.50	1.50	7.6	0.18
IR-17	Dustabad	33.90	0.38	59.18	1.17	7.4	0.41
IR-18	Tabas	33.63	0.29	57.25	0.43	7.1	0.08
IR-19	Golbar-Sirch	30.63	0.89	57.18	0.88	7.1	0.05
IR-20	Nasrata-bad	29.50	0.70	59.60	0.60	7.3	0.23
IR-21	Iran-Pakistan Border	26.97	0.59	61.33	0.47	--	--
PA-1	Makran	24.97	0.41	62.97	0.05	7.8	0.38
PA-2	Ornach Nal	27.02	0.53	65.97	0.04	--	--
PA-3	Chaman	29.83	0.44	66.88	0.83	7.6	0.59
PA-4	NE Afganistan	35.95	0.54	68.00	1.00	7.4	0.30
PA-5	USSR-Afganistan Border	39.03	0.55	70.11	0.99	7.5	0.33
HI-1	Badakh Shan	36.42	1.29	70.83	0.90	--	--
HI-2	Jammu	36.16	0.76	72.86	0.35	--	--
HI-3	Kashmir	32.50	0.52	77.00	1.15	7.4	0.46

Seismogenic Source		$\varphi^{o}N$	$\pm\sigma$	$\lambda^{o}E$	$\pm\sigma$	M_f	P_{10}
HI-4	Gangdise Shan	30.05	0.64	80.08	1.00	7.3	0.04
HI-5	Tangra Yumco	28.47	0.12	83.67	0.94	7.3	0.34
HI-6	Bihar	30.40	0.48	89.97	1.18	7.8	0.40
HI-7	Lhasa	28.96	1.09	94.00	1.10	7.0	0.23
CH-1	Szechwan 1	30.17	0.96	100.5	1.33	7.6	0.48
CH-2	Szechwan 2	31.11	1.15	102.3	1.48	7.7	0.71
CH-3	Tsinghai	36.47	0.76	95.75	1.79	8.0	0.79
CH-4	Lanzou	36.40	0.67	103.7	0.94	7.8	0.47
CH-5	Xining	36.88	1.11	100.5	0.50	7.1	0.01
CH-6	Lenghu	38.12	0.62	93.20	2.32	7.7	0.60
CH-7	Altyn Shan	36.58	0.73	86.00	1.67	7.2	0.42
CH-8	Karakoram	35.80	0.81	79.56	1.71	--	--
CH-9	Tarim Pendi	40.59	0.72	78.33	1.45	7.4	0.35
CH-10	Alma-Ata	43.35	1.05	81.00	3.02	7.8	0.67
CH-11	Junggar Pendi	45.56	1.08	91.00	1.22	7.6	0.46
CH-12	Bajanchongor	44.72	0.76	99.40	1.02	7.2	0.34
CH-13	Changaj Nuruu	48.28	0.70	100.9	2.32	7.3	0.49
CH-14	Beijing	38.40	0.94	116.3	1.54	7.3	0.39
FE-1	Pegu	17.17	1.45	95.44	0.96	7.6	0.36
FE-2	Chin Hills	23.12	0.88	95.22	1.03	7.5	0.45
FE-3	Patkai Range	25.97	0.84	95.95	1.33	7.6	0.67
FE-4	Bangladesh	25.06	0.46	91.50	0.87	7.6	0.56
FE-5	Mishmi Hills	27.63	0.26	101.3	0.83	--	--
FE-6	Yun Nan	25.74	0.98	101.3	0.66	7.3	0.38
FE-7	Shan State	23.17	1.03	99.05	1.00	7.4	0.15
FE-8	Nicobar Isl.	7.70	0.85	93.74	0.67	7.7	0.50
FE-9	Andaman Isl.	12.30	1.49	92.89	1.02	7.7	0.62

DISCUSSION

The basic tenet of the time and magnitude predictable model applied in the Alpine-Himalayan belt, that is, that the recurrence interval and the magnitude of the preceding main shock are positevely correlated, seems to be valid.

There are, however, some constraints on the resolution capability of the model, which have their origin in two factors of uncertainties that inevitably introduce errors. These factors are not considered in the model and concern the long-term clustering of earthquakes and the stress interaction between adjacent areas.

The problem of long-term clustering of earthquakes is difficult to be solved. Ambraseys and Melville (1982) note that if a stationary process is assumed while in fact the seismicity is broadly clustered, the deduced frequency distribution will either overestimate or underestimate future activity, depending on whether the sample of observations was taken from a high or low period of current activity. Clustering process is suggested by Sieh et al. (1989) after paleoseismic studies at Palette Creek, California, although a Poisson process cannot be rejected. Kagan and Jackson (1991a, b) conclude that earthquakes occur in clusters, rather than quasiperiodically. On the other hand, McGuire (1979) and McGuire and Barnhard (1981) examining historical seismicity in China believe that the most recent past may be a better indicator of short-term future seismic activity than the average of data over a very long period, though the most reliable estimate of maximum event is determined by examining the entire catalogue.

Regarding the other source of uncertainties, i.e. the interaction between adjacent faults or the stress transfer between regions, ongoing research concerns both stochastic and deterministic models (Cornell et al., 1993; Zheng and Vere-Jones, 1991). Ward (1991) constructed a model in which fault segment lengths and strengths are adjusted to mimic the actual geography and timing of large historical earthquakes along the Middle America Trench. Recent studies by Stein et al. (1992), who simulated the immediate static response of the crust to earthquakes by using an elastic halfspace boundary element method, seem to give encouraging results.

Both sources of uncertainties exist in the present case and are expressed by the standard deviations in the relations (8) and (9). However, the good fit of these relations to the observational data (Figs. 2-4) indicates that the magnitude of a main shock in a seismogenic source is among the significant factors that govern the time of occurrence and the magnitude of the next main shock in this source.

ACKNOWLEDGEMENTS

The authors thank Drs. E. Scordilis and C. Papazachos for kindly providing the computer codes necessary to complete the data processing (main shock discrimination, multilinear regression). This work was partially supported by EV5V-CT94-0443 contract (C.E.C.).

REFERENCES

ABE, K. (1981). Magnitudes of large earthquakes from 1904 to 1980, Physics Earth Planet. Interiors, 27, 72-93.

ABE, K. (1984). Complements to "Magnitudes of large shallow earthquakes from 1904 to 1980", Physics Earth Planet. Interiors, 34, 17-23.

ABE, K. and NOGUCHI, S. (1983). Revision of magnitudes of large shallow earthquakes, 1897-1912, Physics Earthq. Planet. Interiors, 33, 1-11.

AMBRASEYS, N. N. (1970). Some characteristic features of the Anatolian Fault Zone, Tectonophysics, 9, 143-165.

AMBRASEYS, N.N. and MELVILLE, C.P. (1982). A history of persian earthquakes, Cambridge University press, Cabridge, 219 pp.

AMBRASEYS, N. N. and MELVILLE, C. P. (1988). An analysis of the eastern Mediterranean earthquake of 20 May 1202, in: Historical Seismograms and Earthquakes of the World, W. H. K. Lee, H. Meyers and K. Shimazaki (eds.), Academic Press, San Diego, pp. 181-200.

AMBRASEYS, N. N. and BARAZANGI, M. (1989). The 1759 earthquake in the Bekaa Valley: implications for earthquake hazard assessment in the eastern Mediterranean region, J. Geophys. Res., 94, 4007-4013.

ANDERSON, H. and JACKSON, J. (1987). Active tectonics of the Adriatic region, Geophys. J. R. astr. Soc., 91, 937-983.

BARKA, A. A. and CADINSKY-CADE, K. (1988). Strike-slip fault geometry in Turkey and its influence on earthquake activity, Tectonics, 7, 663-684.

BUFE, C.G., HARSH, P.W. and BURFORD, R.O. (1977). Steady-state seismic slip- a precise recurrence model, Geophys. Res. Letts., 4, 91-94.

BUFORN, E., UDIAS, A. and MEZCUA, J. (1988). Seismicity of focal mechanisms in south Spain, Bull. Seismol. Soc. Am., 78, 2008-2024.

CORNELL, C.A., WU, S., WINTERSTEIN, S.T., DIETERICH J.H. and SIMPSON, R.W. (1993). Seismic hazard induced by mechanically interactive fault segments, Bull. Seismol. Soc. Am., 83, 436-449.

DEWEY, J. W. (1990). The 1954 and 1980 Algerian earthquakes: implications

for the characteristic displacement model of fault behavior, Bull. Seismol. Soc. Am., 81, 446-467.
DRAPER, N.R. and SMITH, H. (1966). Applied regression analysis, Wiley, New York, 407 pp.
GASPERINI, P. and MULARGIA, F. (1992). Statistical analysis of Italian seismicity at regional scale, in: Earthquake Prediction, 5th Course, M. Dragoni and E. Boschi (eds.), Instituto Nazionale di Geofisica, Roma, pp. 417-430.
GUTENBERG, B., and RICHTER, C.F., (1944). Frequency of earthquakes in California, Bull. Seismol. Soc. Am., 34, 185-188.
JACKSON, J. and McKENZIE, D. (1984). Active tectonics of the Alpine-Himalayan Belt between western Turkey and Pakistan, Geophys. J. R. Astron. Soc., 77, 185-264.
JACKSON, J. and McKENZIE, D. (1988). The relationship between plate motions and seismic moment tensors, and the rates of active crustal deformation in the Mediterranean and Middle East, Geophys. J. Int., 93, 45-73.
KAGAN, Y. Y. and JACKSON, D. D. (1991a). Seismic gap hypothesis: ten years after, J. Geophys. Res., 96, 21419-21431.
KAGAN, Y. Y. and JACKSON, D. D. (1991b). Long-term earthquake clustering, Geophys. J. Int., 104, 117-133.
KAILA, K. L., GAUR, V. K. and NARAIN, H. (1972). Quantitative seismicity maps of India. Bull. Seismol. Soc. Am., 62, 1119-1132.
KAILA, K. L., RAO, N. M. and NARAIN, H. (1974). Seismotectonic maps of southwest Asia region comprising eastern Turkey, Caucasus, Persian plateau, Afghanistan and Hindukush, Bull. Seismol. Soc. Am., 64, 657-669.
KANAMORI, H. (1977). The energy released in great earthquakes, J. Geophys. Res., 79, 2981-2987.
KARAKAISIS, G. F. (1993). Time dependent seismicity in Italy, Publ. Geophys. Lab., Univ. of Thessaloniki, pp.18.
KARAKAISIS, G.F. (1994a). Long-term earthquake prediction along the North and East Anatolian Faults Zones based on the time- and magnitude predictable model, Geophys. J. Int., 116, 198-204.
KARAKAISIS, G. F. (1994b). Long-term earthquake prediction in Iran based on the time and magnitude predictable model, Physics Earth Planet. Interiors, pp. 17 (in press).
KARAKAISIS, G.F., KOUROUZIDIS, M. C. and PAPAZACHOS, B. C. (1991). Behaviour of the seismic activity during a single seismic cycle, in Proceedings of the International Conference on Earthquake Prediction: State-of-the-Art, Strasbourg, France, 15-18 October 1991, pp. 47-54.
KIRATZI, A. A. and PAPAZACHOS, C. B. (1994). Seismic crustal deformation along the Azores-Gibraltar region, Publ. Geophys. Lab., Univ. of Thessaloniki, pp.23.
McGUIRE, R.K. (1979). Adequacy of simple probability models for calculating felt-shaking hazard, using the Chinese earthquake catalogue, Bull. Seismol. Soc. Am., 69, 877-892.
McGUIRE, R.K. and BARNHARD, J. (1981). Effects of temporal variations in seismicity on seismic hazard, Bull. Seismol. Soc. Am., 71, 321-334.
McKENZIE, D. (1972). Active tectonics of the Mediterranean region, Geophys. J. R. Astron. Soc., 30, 109-185.
MOLNAR, P. (1979). Earthquake recurrence intervals and plate tectonics,

Bull. Seismol. Soc. Am., 69, 115-133.
MOLNAR, P. and TAPPONNIER, P. (1975). Cenozoic tectonics of Asia: effects of a continental collision, Science, 189, 419-426.
MOLNAR, P. and TAPPONNIER, P. (1978). Active tectonics of Tibet. J. Geophys. Res., 83, 5361-5375.
MOGI, K. (1985). Earthquake Prediction, Academic Press, Japan.
MULARGIA, F., GASPERINI, P. and TINTI, S. (1987). Contour mapping of Italian seismicity, Tectonophysics, 142, 203-216.
NOWROOZI, A.A. (1971). Seismotectonics of the Persian plateau, eastern Turkey, Caucasus, and Hindu-Kush regions, Bull. Seismol. Soc. Am., 61, 317-341.
PACHECO, J. F. and SYKES, L. R. (1992). Seismic moment catalog of large shallow earthquakes, 1900 to 1989, Bull. Seismol. Soc. Am., 82, 1306-1349.
PANAGIOTOPOULOS, D. G. (1994). Long-term earthquake prediction along the seismic zone of Solomon islands and New Hebrides based on the time and magnitude predictable model, Natural Hazards, (in press).
PAPADIMITRIOU, E. E. (1993). Long-term earthquake prediction along the western coast of south and central America based on a time predictable model, Pure Appl. Geophys., 140, 301-316.
PAPAZACHOS, B.C. (1988a). Seismic hazard and long-term earthquake prediction in Greece, European School of Earthquake Sciences, Cource on Earthquake hazard Assessment, 10 pp.
PAPAZACHOS, B. C. (1988b). Long-term earthquake prediction of earthquakes in seismogenic sources of Greece, United Nations Seminar on the prediction of earthquakes, Lisbon, Portugal, pp. 77-84.
PAPAZACHOS, B. C. (1989). A time-predictable model for earthquakes in Greece, Bull. Seismol. Soc. Am., 79, 77-84.
PAPAZACHOS, B. C. (1990). Seismicity of the Aegean and surrounding area, Tectonophysics, 178, 287-308.
PAPAZACHOS, B. C. (1992). A time- and magnitude predictable model for generation of shallow earthquakes in the Aegean area, Pure Appl. Geophys., 138, 287-308.
PAPAZACHOS, B. C. (1993). Long-term earthquake prediction of intermediate depth earthquakes in the southern Aegean region based on a time-predictable model, Natural Hazards, 7, 211-218.
PAPAZACHOS, B. C. and Ch. A. PAPAIOANNOU (1993). Long-term earthquake prediction in the Aegean area based on a time- and magnitude predictable model, Pure Appl. Geophys., 140, 593-612.
PAPAZACHOS, B. C., PAPADIMITRIOU, E. E., KARAKAISIS, G. F. and PANAGIOTOPOULOS, D. G. (1994). Long-term earthquake prediction in the circum-Pacific convergent belt. 27th General Assembly of IASPEI, Wellington, New Zealand, 10-21 January 1994, pp. 39.
QUITTMEYER, R. C. (1979). Seismicity variations in the Makran region of Pakistan and Iran: relation to great earthquakes, Pageoph, 117, 1212-1228.
QUITTMEYER, R. C. and JACOB, K. H. (1979). Historical and modern seismicity of Pakistan, Afghanistan, northwestern India, and southeastern Iran, Bull. Seismol. Soc. Am., 69, 773-823.
SHIMAZAKI, K. and NAKATA, T. (1980). Time-predictable recurrence of large

earthquakes, Geophys. Res. Letts., 7, 279-282.
SIEH, K., STUIVER, M. and BRILLINGER, D. (1989). A more precise chronology of earthquakes produced by the San Andreas fault in southern California, J. Geophys. res., 94, 603-623.
STEIN, R. S., KING, G. C. P. and LIN, J. (1992). Change in failure stress on the southern San Andreas Fault System caused by the 1992 Magnitude=7.4 Landers earthquake, Science, 258, 1328-1332.
SYKES, L. R., and QUITTMEYER, R.C. (1981). Repeat times of great earthquakes along simple plate boundaries, In: D.W. Simpson and P.G. Richards(Editors), Earthquake Prediction, An International Review, Am. Geophys. Union, Maurice Ewing Ser., vol. 4, 297-332.
TAPPONNIER, P. and MOLNAR, P. (1977). Active faulting and tectonics in China, J. Geophys. Res., 82, 2905-2930.
TSAPANOS, T. M., SCORDILIS, E. M. and PAPAZACHOS, B. C. (1990). A global catalogue of strong earthquakes, Publ. Geophys. Lab., Univ. of Thessaloniki, pp. 90.
TSAPANOS, T. M. and PAPAZACHOS, B. C. (1994). Long-term earthquake prediction in China based on the time and magnitude predictable model, J. Earthq. Pred. Res., pp. 26 (in press).
WARD, S. N. (1991). A synthetic seismicity model for the Middle America Trench, J. Geophys. Res., 96, 21433-21442.
WEISBERG, S. (1980). Applied linear regression, Wiley, New York, 238 pp.
ZHANG, S. and CHEN, S. (1989). Structures interpreted from LandSat images, in: Lithospheric Dynamics Atlas of China, China Cartographic Publishing House, pp. 41-44.
ZHENG, X. and VERE-JONES, D. (1991). Application of stress release models to historical earthquakes from North China, Pure Appl. Geophys., 135, 559-576.